EARTH SURFACE PROCESSES AND LANDFORMS
Earth Surf. Process. Landforms **36**, 1590–1603 (2011)

Published online 3 June 2011 in Wiley Online Library
(wileyonlinelibrary.com) DOI: 10.1002/esp.2168

Response of surface processes to climatic change in the dunefields and Loess Plateau of North China during the late Quaternary

Huayu Lu,[1,2]* Joseph A. Mason,[2] Thomas Stevens,[3] Yali Zhou,[4] Shuangwen Yi[1] and Xiaodong Miao[5]
[1] School of Geographic and Oceanographic Sciences, the MOE Key Lab of Coast & Island Development, Nanjing University, Nanjing 210093, China
[2] Department of Geography, University of Wisconsin Madison, WI 53706, USA
[3] Centre for Quaternary Research, Department of Geography, Royal Holloway, University of London, Egham, Surrey TW20 0EX, UK
[4] College of Tourism & Environment, Shaanxi Normal University, Xi'an 710062, China
[5] Illinois State Geological Survey, 615 E. Peabody Dr., Champaign, IL 61820, USA

Received 28 December 2009; Revised 15 March 2011; Accepted 11 April 2011

* Correspondence to: H. Lu, School of Geographic and Oceanographic Sciences, the MOE Key Lab of Coast & Island Development, Nanjing University, Nanjing 210093, China. E-mail: huayulu@nju.edu.cn

ESPL
Earth Surface Processes and Landforms

ABSTRACT: This paper draws on recent optically stimulated luminescence (OSL) dating to evaluate the long-held assumption that dust accumulation rates in the Loess Plateau and the extent of active aeolian sand in the dunefields to the north have varied together over time, because both are controlled by the strength of the Asian monsoons and also possibly because the dunefields are proximal loess sources. The results show there is little evidence that high rates of loess accumulation coincided with well-dated episodes of extensive dune activity in the Mu Us, Otindag, and Horqin dunefields, at 11–8 ka and 1–0 ka. Explanations for the apparent lack of coupling include local variation in the trapping of dust and post-depositional preservation of the loess and dune sediments, in response to varying local environmental conditions. In addition, a substantial portion of the loess may be transported directly from source areas where dust emission has somewhat different climatic and geomorphic controls than aeolian sand activity within the dunefields. The results of this study cast doubt on the use of loess accumulation rate as a palaeoclimatic proxy at millennial timescale. The dunefield and loess stratigraphic records are interpreted as primarily recording changes in effective moisture at a local scale, but the timing of late Quaternary dune activity, along with a variety of other evidence, indicates that moisture changes in many of the drylands of northern China may not be in phase with precipitation in core regions of the Asian monsoons. Copyright © 2011 John Wiley & Sons, Ltd.

KEYWORDS: dunefield; loess; loess provenance; dust accumulation rate; OSL dating; late Quaternary; northern China; Asian monsoon

Introduction

The aeolian sands and loess deposits of North China form one of the best-known aeolian systems in the world, covering an area of approximately 2×10^6 km^2 within the extensive drylands of central Asia. In this region, loess deposits are typically limited to subhumid and semiarid climates, while the dunefields occur in semiarid to arid regions north and north-west of the major loess deposits (Liu, 1964, 1985). It is widely suggested that climatically driven changes in dunefield activity and the accumulation rate of dust in the Loess Plateau are tightly coupled, both responding to changes in the strength of the Asian monsoons (Liu and Ding, 1998; Porter, 2001; Dong, 2002). That is, when the northward extent of summer monsoon rainfall is reduced, the area of active dunes should expand and more dust should be produced in the dunefields and other desert regions north and north-west of the Loess Plateau, resulting in higher loess accumulation rates. Prior work has often focused on orbital timescales, with major periods of relatively rapid loess accumulation and desert expansion occurring during glacial periods, and slower accumulation and desert contraction during interglacial periods when the summer monsoon was strengthened. However, despite a long history of research on the aeolian landscapes, this conceptual model has not been adequately tested, particularly at millennial to multi-millennial timescales.

It is important to recognize that dune activity and loess accumulation may be linked in two distinctly different, but not mutually exclusive ways. First, both dune activity and dust production in the loess source areas may represent responses to climatic changes that were potentially contemporaneous in both regions, especially changes in the summer monsoon precipitation and the strength of the winter monsoon winds flowing out of the Siberian High (Liu and Ding, 1998). For this type of linkage, we would expect that rapid loess accumulation and extensive dune activity would be broadly synchronous *if* both aeolian sand and loess systems respond strongly to similar climatic factors *and* neither system is significantly affected by

variation of sediment supply over time. Limitation by sediment supply could cause asynchronous behavior; for example, depletion of silt-size material in loess source regions could result in lower accumulation rates downwind while dunes remained active, even if climatic conditions were still favorable for both dust production and dune activity.

Second, dust generated within the dunefields as a result of enhanced aeolian activity could make a substantial contribution to the total dust influx to the Loess Plateau, so changes in dune activity influence the loess accumulation rate. It is widely accepted that the 'sand-blasting' effects of saltating sand can yield high rates of dust emission if sufficient fine material is exposed where saltation is active (Nickling and Gillies, 1989; Shao *et al.*, 1993). Thus, dust deposited in the dunefields of northern China may be trapped and stored there during periods of partial or full stabilization of the dunes and then released at high rates when the dunes are reactivated, resulting in a peak of loess accumulation downwind. There is also evidence that silt produced within dunefields by abrasion of the saltating sand grains contributes to some loess deposits (Smalley and Vita-Frinzi, 1968; Wright *et al.*, 1998; Wright 2001, 2007; Bullard *et al.*, 2004, 2007; Crouvi *et al.*, 2008), although it seems unlikely that this process could operate at high enough rates to produce much of the vast quantity of loess accumulated in north China during the late Quaternary. For this second type of linkage, synchronous dune activity and rapid loess accumulation would also be expected, in the absence of major sediment supply effects. In particular, sustained, rapid loess accumulation would depend on a large supply of silt stored in the dunes, new influx of silt to the dunefields from more distant sources, and/or abundant sand grains susceptible to abrasion within the dunefields. Otherwise, the rate of loess accumulation would decrease well before dune activity ceased.

In this study, we evaluate the relationship between surface processes in the dunefields and the Loess Plateau using data from four late Quaternary loess-paleosol sequences in the Chinese Loess Plateau, and 23 stratigraphic sections in dunefields (Figures 1–3). New optically stimulated luminescence (OSL) ages are presented here and are added to our previously reported datasets (Lu *et al.*, 2005; Stevens *et al.*, 2006, 2008; Zhou *et al.*, 2008; Mason *et al.*, 2009) (Tables I, II).

Geographical Setting and Methods

The sand and loess deposits investigated in this study are located in the Mu Us, Otindag, and Horqin dunefields of northern China and the Chinese Loess Plateau (Figure 1). The dunefields are semiarid, with mean annual precipitation of 250–450 mm yr^{-1}, and are used mainly as rangeland. Substantial areas of stabilized dunes do not occur in more humid areas beyond the southern margins of these dunefields; therefore those margins mark the approximate maximum extent of late Quaternary expansion of dune activity in northern China. In test areas located within the dunefields, classification of Landsat images indicates that about 5% to 35% of the land surface is bare, active aeolian sand, while much of the remainder is occupied by vegetation-stabilized dunes or sand sheets (Mason *et al.*, 2008). Typical dune morphologies are described and illustrated by Mason *et al.* (2008). Fully active dunes in the Mu Us region are generally barchanoid or transverse ridges (5–15 m high), but stabilized dunes of this type have not been identified. Vegetation-covered areas of older sand form closely spaced simple parabolic dunes or hummocky sand sheets. The Otindag dunefield is dominated by large compound parabolic dunes (up to at least 20 m high and several km long), ranging from fully vegetation-stabilized to a state in which scattered vegetation may remain on the upwind arms of the dune, but much of the dune surface is bare sand. Much of the Horqin dunefield is covered by vegetation-stabilized simple or compound parabolic dunes and sand sheets. Small patches of fully active transverse ridge or barchan dunes occur in the Otindag dunefield, and larger patches of fully active barchans,

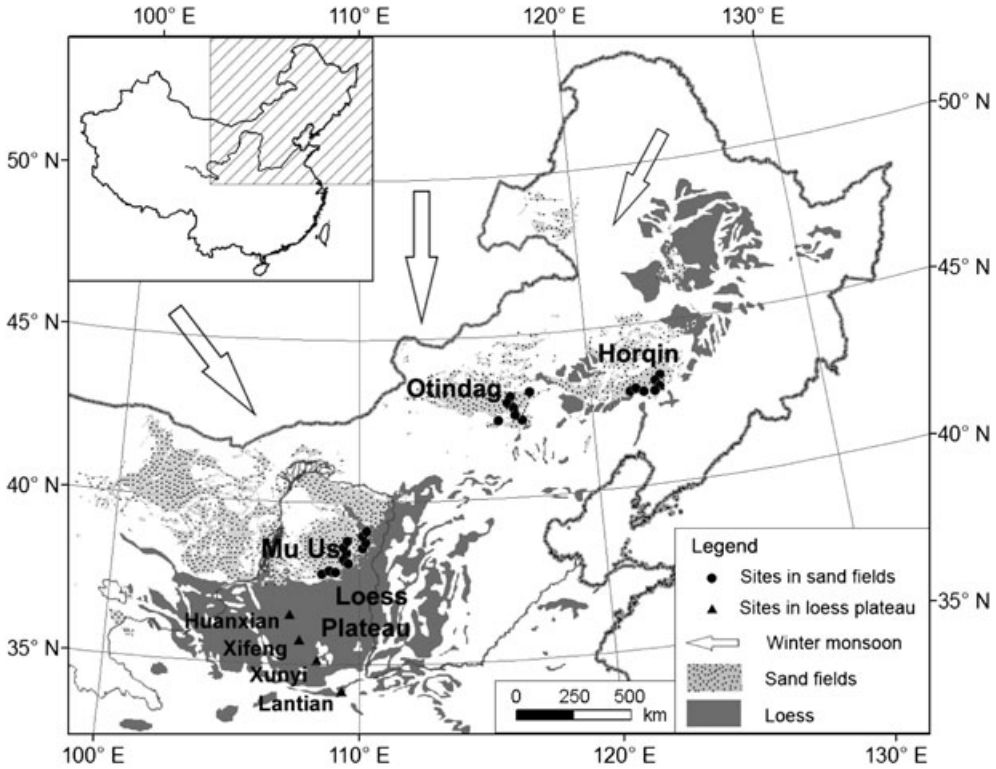

Figure 1. Map of the study area and sampled sites in the dunefields and the Loess Plateau of northern China.

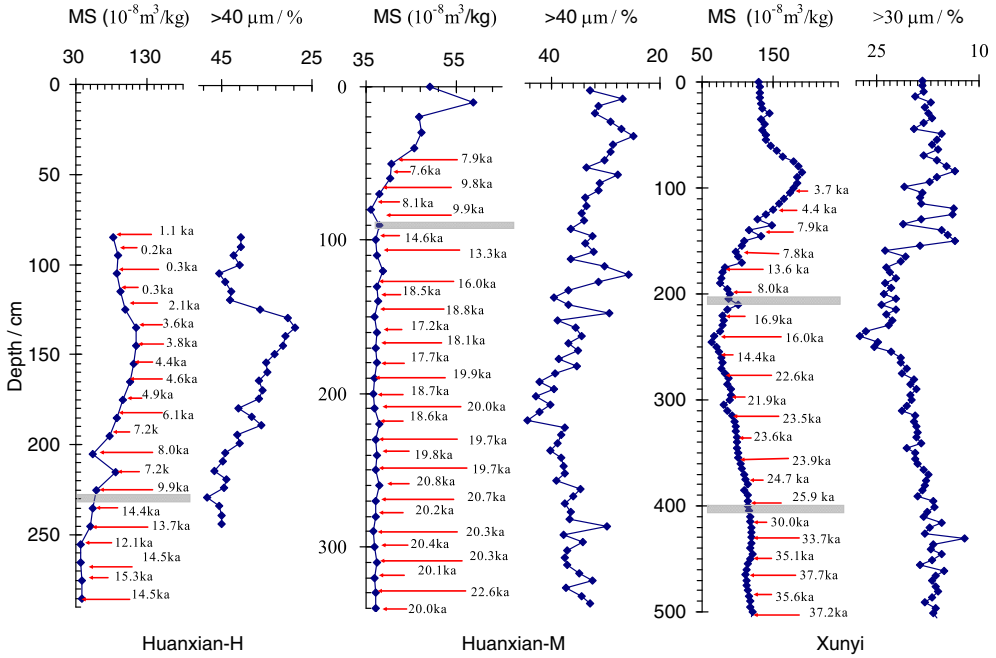

Figure 2. Variations of magnetic susceptibility and grain-size of the loess-paleosol sequences at Huanxian, Xifeng, Xunyi and Lantian sampling sites in the Chinese Loess Plateau, with OSL ages. This figure is available in colour online at wileyonlinelibrary.com/journal/espl

barchanoid ridge, and longitudinal dunes are common in the Horqin dunefield, but no stabilized dunes of these types have been identified in either area. The climate of the Loess Plateau, which has an area of 360,000 km^2 (Li and Lu, 2010), varies from subhumid in the south (mean annual precipitation of 500–700 mm yr^{-1}) to semiarid in the north (200–400 mm yr^{-1}).

The sections within dunefields were sampled using artificial or natural exposures, allowing detailed characterization of stratigraphy, sedimentary structures, and soil horizons, with augering used in a few cases to investigate stratigraphy below the exposure face. Sampling was based on stratigraphy, that is, the primary goal was to date discrete units of clearly identifiable aeolian sand bounded by paleosols, truncation surfaces, or non-aeolian sediment, where possible dating upper and lower parts of each unit. In some sections, we also collected OSL dating samples from within paleosols; interpretation of these soil ages is discussed below. The newly reported OSL ages in this paper are presented in Table I, while Table II combines these with previously reported OSL ages (Lu *et al.*, 2005; Zhou *et al.*, 2008; Mason *et al.*, 2009) to summarize age constraints on dune activity. The loess-paleosol sequences were sampled at 10–20 cm intervals and the samples were measured for OSL dating, grain-size distribution and magnetic susceptibility, the results have been reported (Lu *et al.*, 2006; Stevens *et al.*, 2006, 2008) and will have more discussions in this paper.

The newly reported OSL ages were produced in the Nordic Laboratory for Luminescence Dating (labeled EDxxx in Table I), the Luminescence Geochronology Laboratory of University of Nebraska (labeled UNL-xxxx in Table I) and at Peking University (labeled PKU-xxxx in Table I), with similar methods used in each case. Tubes were inserted into cleaned sediment faces to obtain samples without light exposure. Samples from the sunlight-exposed ends of each tube were scraped away under subdued amber light. The unexposed part was prepared for equivalent dose (De) determination and the exposed part was retained for radioisotope and *in situ*

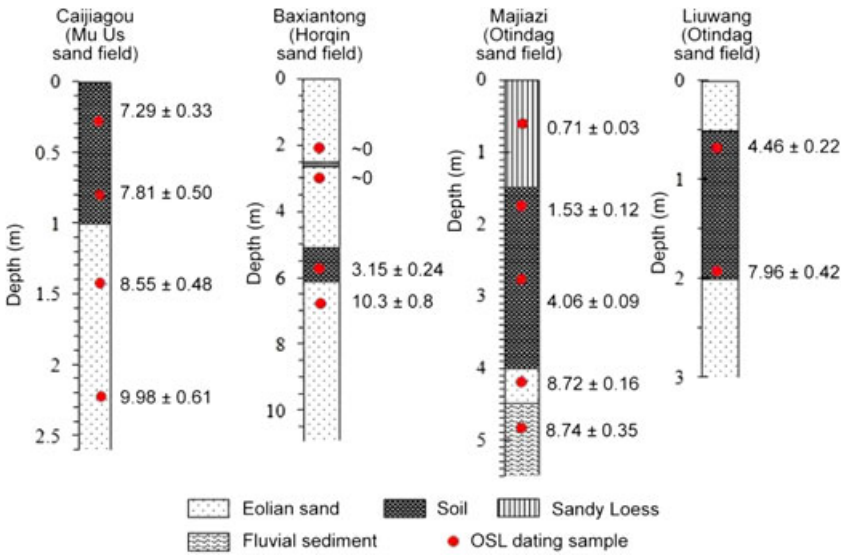

Figure 3. Representative stratigraphic sections from the three dunefields, with OSL ages, illustrating typical lithofacies and OSL sampling strategy. This figure is available in colour online at wileyonlinelibrary.com/journal/espl

Table I. List of previously unpublished OSL ages and associated data

Study site and Lab No.	Depth (m)	*In situ* H_2O (%)	U (Bq/kg)	Th (Bq/kg)	K (Bq/kg)	Cosmic (Gy/ka)	Dose rate (Gy/ka)	Dose (Gy/ka)	Aliquots (n)	Age (ka)
Sangan Dalai South-B (Otindag sand field)										
ED650	2.2	1.86	7.40	9.00	723	0.20	2.75 ± 0.13	7.60 ± 0.14	15	2.76 ± 0.15
ED651	3.1	2.54	8.90	9.35	754	0.18	2.81 ± 0.13	12.62 ± 0.25	15	4.48 ± 0.24
ED652	6.3	18.28	14.00	9.18	383	0.12	1.42 ± 0.06	25.15 ± 0.50	15	17.7 ± 0.9
207 Road 116 km (Otindag sand field)										
ED653	1.0	1.34	22.00	9.04	746	0.23	2.94 ± 0.14	1.44 ± 0.06	15	0.49 ± 0.03
303 Road 1100 km (Otindag sand field)										
ED654	0.6	30.85	16.00	14.60	776	0.25	2.44 ± 0.09	36.73 ± 0.67	15	15.1 ± 0.7
ED655	1.2	23.82	12.00	22.00	346	0.24	1.63 ± 0.07	38.48 ± 0.77	15	23.7 ± 1.2
			U (ppm)	Th (ppm)	K (%)					
Majiazi (Otindag sand field)										
PKU-L223	0.7	0.53	0.49	1.78	2.82	0.22	3.12 ± 0.00	2.2 ± 0.1	12	0.705 ± 0.03
PKU-L224	1.8	1.46	0.62	3	2.8	0.19	3.21 ± 0.01	4.9 ± 0.4	12	1.53 ± 0.02
PKU-L225	2.8	1.66	0.66	3.69	2.73	0.17	3.18 ± 0.01	12.9 ± 0.3	18	4.06 ± 0.09
PKU-L226	4.2	2.70	0.50	2.00	2.98	0.14	3.21 ± 0.00	28.0 ± 0.5	12	8.72 ± 0.16
PKU-L227	4.8	1.49	0.79	4.33	2.63	0.13	3.17 ± 0.01	27.7 ± 1.1	12	8.74 ± 0.35
Shijiajia (Mu Us sand field)										
UNL-914	1.0	6.4	2	10.4	1.78	0.2	2.93 ± 0.15	47.4 ± 2.5	16	16.2 ± 1.3
			U (ppm)	Th (ppm)	K_2O (%)					
Sangan Dalai North (Otindag sand field)										
UNL-1222[a]	0.5	0.7	0.5	2.0	2.65	0.23	2.68 ± 0.10	0.35 ± 0.02	25	0.13 ± 0.01
Baxiantong (Horqin sand field)										
UNL-1252[b]	2.9	2.02	0.5	2.2	2.46					~0
UNL-1253[a]	5.4	6.49	0.8	3.7	2.49	0.10	2.36 ± 0.15	7.43 ± 0.90	20	3.15 ± 0.24
UNL-1254[a]	6.8	1.91	0.4	1.7	2.02	0.09	1.87 ± 0.13	19.32 ± 2.65	23	10.3 ± 0.8
Bahuta (Horqin sand field)										
UNL-1255[b]	17.0	6.67	0.4	1.6	2.34					~0
Sanjianzi (Horqin sand field)										
UNL-1256[a]	1.9	5.13	0.8	4.0	2.87	0.16	2.77 ± 0.18	2.09 ± 0.11	16	0.76 ± 0.05
UNL-1257[a]	3.0	7.15	0.8	4.6	2.96	0.14	2.78 ± 0.18	54.38 ± 6.84	20	19.6 ± 1.5
Bahuta B (Horqin sand field)										
UNL-1258[b]	5.1	6.34	0.4	1.9	2.4					~0
UNL-1259[a]	9.3	4.89	0.4	2.0	2.53	0.07	2.19 ± 0.15	22.34 ± 3.12	19	10.2 ± 0.8
Shalilai (Horqin sand field)										
UNL-1260[b]	7.4	3.36	0.4	1.7	2.79					~0
UNL-1261[a]	15.8	11.21	0.3	1.6	2.43	0.04	1.90 ± 0.15	20.55 ± 1.73	18	10.8 ± 0.9
Yuanyichang (Mu Us sand field)										
CHO2/22/2[c]										2.39 ± 0.14
CHO2/22/3[c]										0.29 ± 0.05

[a]UNL-1222, -1253, -1254, -1256, -1257, -1259, and −1261 are reported in Mason *et al.* (2009).
[b]Preliminary OSL measurements on UNL-1252, -1255, -1258, and −1260 indicated they were very close to modern, so no further analysis was undertaken (stratigraphic context is consistent with very recent deposition in all cases).
[c]CHO ages provided by Stephen Stokes, Oxford University, with no associated data.

water content analysis. The pretreatment process included removing carbonates and organics by HCl (10%) and H_2O_2 (30%) respectively, wet sieving to extract the 63–105 μm or 90–125 μm particle fraction, heavy liquid ($\rho = 2.70$ g cm^{-3}) separation to remove heavy minerals such as zircon, etching using HF (40%) for 40 min to remove feldspars, immersion in 10% HCl to remove fluoride precipitates, and re-sieving. The purity of quartz grains was examined by observing the infrared-stimulated luminescence (IRSL) signal and the shape of the 110 °C TL peak; impure samples were pretreated by HF again until pure quartz particles were obtained. Quartz grains were mounted as a monolayer with a 5 mm spray mask on 9.8 mm diameter aluminum disks using silicone spray oil.

Equivalent doses were measured using the SAR protocol (Murray and Wintle, 2003) on an automated Risø TL/OSL-DA-15B reader, using two 3 mm Hoya U-340 filters in front of a 9235QA photomultiplier tube. The dose rate was calculated from concentrations of U, Th, and K, determined by inductively coupled plasma-mass spectrometry (ICP-MS), neutron activation analysis, and/or laboratory gamma spectrometry (Murray *et al.*, 1987). Sample radioisotope compositions from individual locations are generally consistent. A total error estimate incorporates an assumed error of ±10% in the chemical analyses, or as in the case of ICP-MS, is obtained through repeat measurements. The cosmic ray contribution to the dose rate was calculated from the burial depth, longitude, latitude and elevation of the sample (Prescott and Hutton, 1994). *In situ* water content was measured to correct for its attenuating effect on dose rate, with an assumed relative variation of ±10%. Full details of equivalent dose and dosimetry data are presented in Table I.

Grain-size distribution and magnetic susceptibility of the loess-paleosol sequences used to infer palaeoclimatic conditions were measured by the Malvern Mastersizer 2000 and the Bartington MS2 Meter, respectively, and are presented in Figure 2 (the OSL ages are from Stevens *et al.*, 2006, 2008).

Table II. List of all sandfield ages, with stratigraphic context and references for full details on methodology and sampling sites

Sample Lab Number	Age (ka)	Error (±ka)	Stratigraphic context			Position Within Unit			Reference
			Soil	Loess	Sand	Upper	Middle	Lower	
UNL-1252	~0				√				This paper, Table I
UNL-1255	~0				√				This paper, Table I
UNL-1258	~0				√		√		This paper, Table I
UNL-1260	~0				√	√			This paper, Table I[a]
UNL-913	0.11	0.05			√		√		Lu et al., 2005
UNL-1222	0.13	0.01			√			√	This paper, Table I[a]
PKU-L219	0.15	0.00			√	√			Zhou et al., 2008
CH02/22/3	0.29	0.05			√	√			This paper, Table I
UNL-1229	0.43	0.03			√			√	Zhou et al., 2008
ED-652	0.49	0.03			√	√			This paper, Table I
UNL-1223	0.63	0.04	√					√	Zhou et al., 2008
UNL-1227	0.63	0.04			√		√		Zhou et al., 2008
UNL-1228	0.63	0.04			√			√	Zhou et al., 2008
UNL-1230	0.66	0.04			√	√			Zhou et al., 2008
UNL-1224	0.68	0.04			√		√		Zhou et al., 2008
PKU-L223	0.71	0.03		√			√		This paper, Table I
UNL-1248	0.74	0.04			√			√	Zhou et al., 2008
UNL-1256	0.76	0.05			√		√		This paper, Table I[a]
UNL-1249	0.95	0.05			√		√		Zhou et al., 2008
UNL-908	0.95	0.14	√				√		Lu et al., 2005
UNL-1231	1.30	0.07	√			√			Zhou et al., 2008
PKU-L224	1.53	0.12	√			√			This paper, Table I
UNL-1233	1.62	0.09	√			√			Zhou et al., 2008
UNL-1243	2.34	0.12			√			√	Zhou et al., 2008
CH02/22/2	2.39	0.14	√					√	This paper, Table I
UNL-907	2.67	0.40	√			√			Lu et al., 2005
PKU-L220	2.74	0.06	√			√			Zhou et al., 2008
ED-650	2.76	0.15			√		√		This paper, Table I
UNL-1253	3.15	0.24	√			√			This paper, Table I[a]
UNL-1225	4.04	0.22	√					√	Zhou et al., 2008
PKU-L225	4.06	0.09	√				√		Lu et al., 2005
UNL-1241	4.46	0.22	√			√			Zhou et al., 2008
ED-651	4.48	0.24	√				√		This paper, Table I
UNL-1244	4.97	0.27			√	√			Zhou et al., 2008
PKU-L221	5.02	0.38	√				√		Lu et al., 2005[b]
UNL-910	5.09	0.74			√			√	Lu et al., 2005
UNL-1245	5.24	0.28			√			√	Zhou et al., 2008
UNL-1246	6.64	0.37			√	√			Zhou et al., 2008
CH02/26/1	7.20	0.43		√				√	This paper, Table I
UNL-912	7.23	0.76	√			√			Lu et al., 2005
UNL-906	7.25	1.23			√	√			Lu et al., 2005
PKU-L215	7.29	0.33	√			√			Lu et al., 2005[b]
UNL-679	7.39	0.48	√			√			Lu et al., 2005
PKU-L209	7.56	0.58	√					√	Lu et al., 2005[b]
PKU-L222	7.79	0.20			√	√			Zhou et al., 2008
PKU-L216	7.81	0.50	√					√	Lu et al., 2005[b]
UNL-1242	7.96	0.42	√					√	Zhou et al., 2008
UNL-1250	8.21	0.44		Lake sediment		√			Zhou et al., 2008
PKU-L210	8.10	0.57		√		√			Lu et al., 2005[b]
UNL-1232	8.33	0.46			√	√			Zhou et al., 2008
PKU-L211	8.38	0.55		√				√	Lu et al., 2005[b]
PKU-L217	8.55	0.48			√	√			Lu et al., 2005[b]
UNL-1234	8.68	0.47			√	√			Zhou et al., 2008
PKU-L226	8.72	0.16			√	√			This paper, Table I
PKU-L227	8.74	0.35		Fluvial sand				√	This paper, Table I
UNL-905	8.74	1.37			√			√	Lu et al., 2005
UNL1247	8.88	0.47			√				Zhou et al., 2008
UNL1235	9.37	0.50			√		√		Zhou et al., 2008
PKU-L212	9.81	0.36			√				This paper, Table I
UNL-1226	9.90	0.55			√	√			Zhou et al., 2008
PKU-L218	9.98	0.61			√			√	Lu et al., 2005[b]
UNL-1259	10.2	0.8	√					√	This paper, Table I
UNL-1254	10.3	0.8			√	√			This paper, Table I
UNL-911	10.5	1.7			√	√			Lu et al., 2005
UNL-1261	10.8	0.9			√	√			This paper, Table I

(*Continues*)

Table 2. (Continued)

Sample Lab Number	Age (ka)	Error (±ka)	Stratigraphic context			Position Within Unit			Reference
			Soil	Loess	Sand	Upper	Middle	Lower	
PKU-L213	11.0	0.8			√			√	Lu et al., 2005[b]
UNL-909	11.6	1.6	√					√	Lu et al., 2005
UNL-680	12.7	1.1			√	√			Lu et al., 2005
UNL-681	13.7	1.5			√		√		Lu et al., 2005
ED-654	15.1	0.7		Lake sediment		√			This paper, Table I
UNL-914	16.2	3.5	√			√			Lu et al., 2005
ED-652	17.7	0.9	√				√		This paper, Table I
UNL-904	18.7	2.4		√		√			Lu et al., 2005
UNL-1257	19.6	1.5			√	√			This paper, Table I[a]
ED-655	23.7	1.2		Lake sediment				√	This paper, Table I
UNL-682	37.7	2.8		√		√			Lu et al., 2005
PKU-L214	41.8	2.6		√		√			Lu et al., 2005[b]
UNL-683	52.1	4.0			√	√			Lu et al., 2005
UNL-684	57.1	4.8			√			√	Lu et al., 2005

[a]Ages are in Table Ibut have also been published in Mason *et al.* (2009)
[b]Ages recalculated, slightly changing values, after original publication in Lu *et al.* (2005). See Zhou *et al.* (2009) for details.

Results

OSL chronology from the dunefields

Examples of dunefield sections are illustrated in Figure 3, to complement the sections shown in previous publications (Lu *et al.*, 2005; Zhou *et al.*, 2008; Mason *et al.*, 2009). Aeolian sand, loess, and other sediments were distinguished on the basis of grain size, landscape setting, and where possible, diagnostic sedimentary structures. Soils were identified on the basis of dark-colored (10YR 2/2 to 4/3) buried A horizons and other pedogenic features.

Aeolian sand units were typically well-sorted, light-colored fine sand (moist Munsell colors of 10YR 5/3 to 10YR 7/4), and were often more than 1 m thick. Well-preserved wind-ripple lamination was often observed in at least the lower part of thick sand units. Evidence of bioturbation, such as insect burrowing, is generally concentrated in the upper meter of thick sand units, especially where a soil marks the upper boundary. Where multiple OSL ages were obtained from a single thick aeolian sand unit, they are consistent with rapid deposition (e.g. Caijiagou, Figure 3, and sections in Mason *et al.*, 2009, Figure 2). Taken together, these observations indicate that most of the sand units sampled represent substantial aeolian sand transport and deposition under conditions of minimal vegetation cover, with bioturbation occurring mainly after the bulk of the unit was deposited and subsequently stabilized by vegetation.

Interpretation of the OSL ages from dunefield soils is a more complex problem, because the age may record either the time of deposition, or light exposure through bioturbation at a later date. A few ages from surface soils or buried paleosols are only a little younger than ages from underlying sand, and could represent aeolian deposition before surface stabilization and pedogenesis (e.g. ages within the soil at Caijiagou, Figure 2). In other cases, ages from upper parts of thick soils are thousands of years younger than ages near the base of the soil or in underlying sand, such as the Dabianyao (DBY) site in the southern Mu Us dunefield (Lu *et al.*, 2005). This observation implies either slow sediment accumulation in minor increments that were incorporated into the soil as it developed, light exposure through bioturbation, or a mixture of the two, as discussed for other settings by Goble *et al.* (2004) and Chase and Thomas (2006). In either case, ages within a paleosol should fall between the time the soil parent material was deposited and the time of soil burial by renewed rapid sand deposition.

The OSL ages from all three dunefields are summarized in Figure 4, with all ages and their context listed in Table II. Sediments older than 14 ka were found at several localities. These older sediments are too sparse for more detailed interpretation at this point, but clearly indicate the potential for reconstruction of long-term change in dunefield environments if they can be identified at more localities in the future. A thick aeolian sand unit in the Mu Us dunefield yielded ages of 57.1 ± 4.8 and 52.1 ± 4.0 ka, and is overlain by coarse loess dated to 41.2 ± 2.1, followed by aeolian sand with ages of 13.7 ± 1.5 and 12.7 ± 1.1. Loess at another Mu Us dunefield locality produced a similar age of 37.7 ± 2.8 ka. Younger loess (18.7 ± 2.4 ka) at a third site is directly overlain by early Holocene sand. Lacustrine sediment was deposited above modern interdune levels in the Otindag dunefield at 23.7 ± 1.2 and 15.1 ± 0.7 ka, suggesting quite different hydrologic conditions than at present. A single age of 19.6 ± 1.5 ka records possible aeolian sand deposition in the Horqin dunefield (diagnostic sedimentary structures were not observed in this sample).

Many aeolian sand ages from numerous sites fall within two younger intervals, 11 to 8 ka and the last 1000 years. In all three dunefields, cross-strata recording deposition on dune slipfaces were observed in some of the depositional units of yielding ages of 11 to 8 ka. These units often occur below a prominent dark-colored soil (Caijiagou and Baxiantong, Figure 3). Ages from within this soil fall mostly between 8 and 2 ka (Figure 4b), the soil is frequently buried by late Holocene or modern aeolian sand, and it is also often truncated by erosion when traced laterally. Thus, we interpret the dark soil as a partially preserved land surface of middle Holocene age. This land surface cannot be traced far enough to reconstruct the dune forms active at 11–8 ka, but it is likely that some of the fully stabilized parabolic dunes in the Horqin and Mu Us region are relicts from that time period. In the Otindag dunefield, middle Holocene soils and thick underlying early Holocene sands were sampled from exposures in large compound parabolic dunes, several meters or more above interdune level.

The many ages <1 ka are mostly from currently or recently active dunes, and at several sites they clearly represent deposition on mobile, migrating dunes rather than local surface activation. For example, samples UNL-1227 and −1228, with virtually identical ages of 0.63 ± 0.04 ka (Table II) are from depths of 6 m and 8 m in a new roadcut through the downwind nose of a large, eastward-migrating parabolic dune. Aeolian cross-strata exposed in the roadcut, including the sand dated by

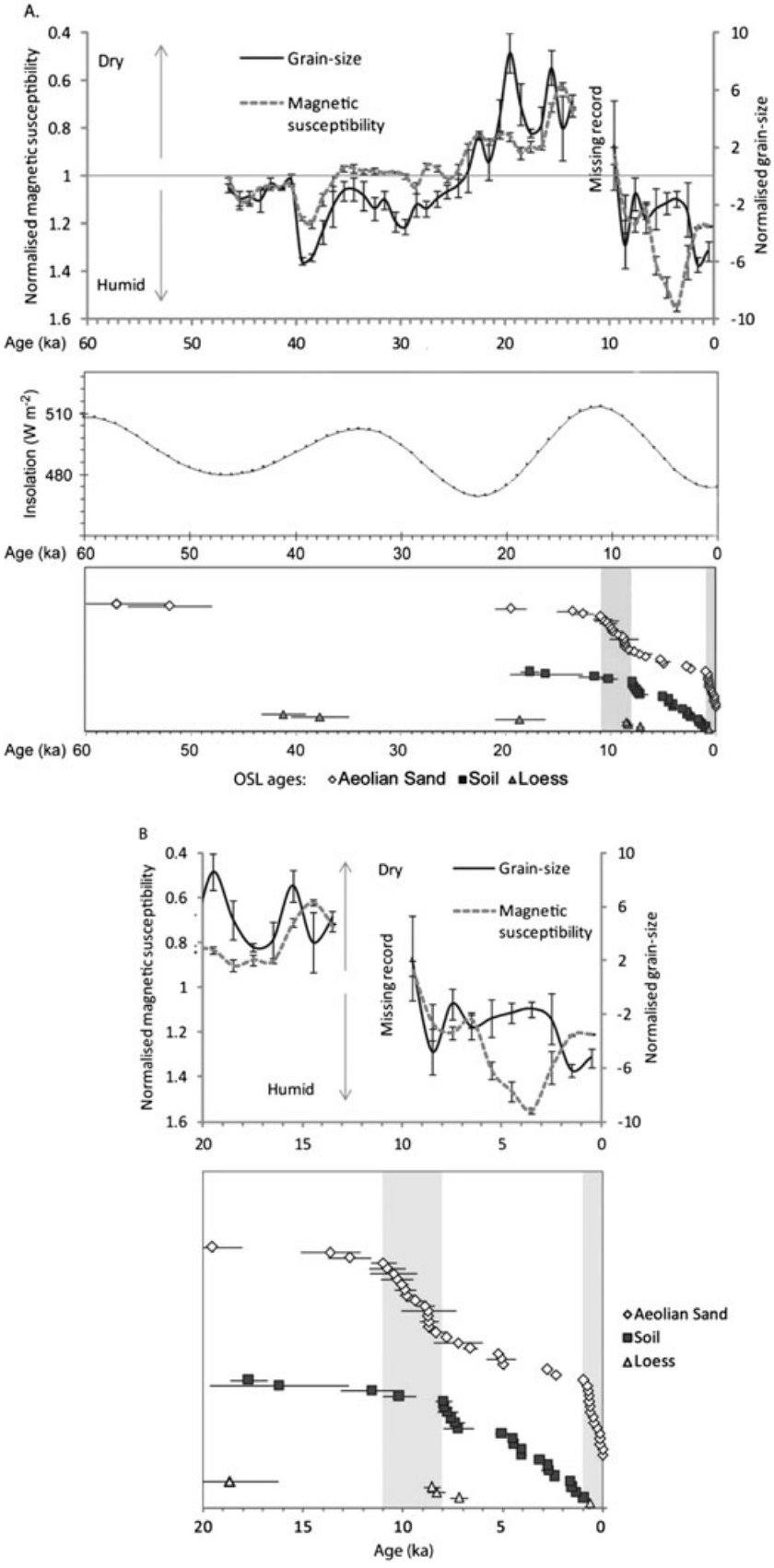

Figure 4. Composite record of dunefield activity and stability, based on OSL dating. Dunefield record is compared with moisture changes inferred from stacked normalized grain-size (% > 30 μm) and magnetic susceptibility (high frequency) records plotted by OSL date with data averaged over 1 kyr intervals in the Loess Plateau (Stevens and Lu, 2009; 2010) and summer insolation at 30°N, often considered to be the key control of monsoon circulation strength. Grain-size record is normalized by taking the difference from average value for each section while magnetic susceptibility is normalized by dividing by the average value for each section. Error bars are 1σ. A. Loess-derived proxy data (top), insolation (middle), and OSL ages from aeolian sand, soils, and loess at dunefield study sites, plotted with ± 1 σ errors (bottom, four near-modern ages that were not fully analyzed are not included; Table I). Ages in each stratigraphic context are ordered vertically from oldest (top) to youngest (bottom). Two vertical gray bars indicate major periods of extensive dune activity and inferred dry climate in the dunefields. B. Expanded view of proxy data and dunefield OSL ages over last 20 kyr; gray bars indicate major periods of dune activity as in A.

UNL-1227, were deposited on slipfaces advancing eastward; thus, the ages probably represent migration of the dune as a whole.

In addition to the major age clusters, a total of six aeolian sand ages are distributed fairly evenly across the interval from 8 to 4 ka (Figure 4b), three of them from a single section within a large compound parabolic dune in the Otindag dunefield (illustrated in Figure 2 of Mason *et al.*, 2009). Other research groups have reported OSL ages that are generally consistent with the patterns identified in our data, from several sites in the Mu Us, Otindag, and Horqin dunefields (Li *et al.*, 2002; Sun *et al.*, 2006; Yang *et al.*, 2008; Ma *et al.*, 2011). In addition, our interpretation of widespread soil development in the middle Holocene is supported by radiocarbon ages from paleosols in the Mu Us dunefield (Yang *et al.*, 2004).

OSL-dated accumulation rate variation in loess deposits

A review of mass accumulation rates of Chinese Loess Plateau revealed discrepancies between those calculated using independent numerical dating of individual loess sections and ages estimated by stratigraphic correlation (Kohfeld and Harrison, 2003). This observation implies a need for detailed numerical dating in determining loess accumulation rates over the last glaciation and Holocene. OSL dating currently offers the best possibility to reconstruct loess accumulation rates on such timescales (Lai *et al.*, 2007; Lu *et al.*, 2007; Buylaert *et al.*, 2008; Stevens and Lu, 2009). While some of the loess sections considered here have been described in a previous paper (Lu and An, 1998), sufficient independent age control to resolve the chronology and accumulation rates at millennial timescales has until recently been absent. Here, our recent detailed OSL dating at a sampling interval of 10–20 cm (Stevens *et al.*, 2006, 2008) offers good constraints to calculate loess accumulation rates using interpolation between two age points or linear regression over a series of ages (Figure 2).

The OSL age models also allow palaeoclimatic proxies such as grain-size and magnetic susceptibility to be plotted on an independent timescale (Stevens and Lu, 2009, 2010). This in turn allows records from multiple sites dated via detailed OSL methods to be stacked together to create a curve of average proxy variation. Due to systematic variation in these parameters across the Loess Plateau this can only been achieved after proxy variation is normalized to site means (Figure 4). This curve will necessarily smooth out millennial scale changes recorded at the sites but will show any longer-term trends in the proxies that are recorded across the Loess Plateau. This approach has been applied before using ages estimated by stratigraphic correlation (Ding *et al.*, 2002). Magnetic susceptibility is widely used as a proxy for intensity of soil formation, and in some cases, as a proxy for rainfall (Liu and Ding, 1998; Maher and Hu, 2006). Grain size is considered variously as a proxy for wind speed or source proximity, often interpreted as being tied to winter monsoon variation and thus correlated with aridity in northern China (Lu and An, 1998; Porter, 2001); however, recent work suggests that the relationship between strong dust-transporting winds and winter monsoon strength is not as simple as previously assumed (Roe, 2009). Although a variety of factors may affect magnetic susceptibility and grain size, the striking similarity between the two (Figure 2 and Figure 4), suggests that they respond to similar broad-scale changes in climate.

Accumulation rate at the sites appears to vary dramatically both within and between sections. Average accumulation rate can vary abruptly by one to two orders of magnitude, even within a single section (Figure 5), although the precise values at high accumulation rates are difficult to calculate due to errors on ages and regression equations with shallow line slope coefficients. Ages from Huanxian section on the northern Loess Plateau, indicate intervals of very rapid dust accumulation centered on about 29 ka, 25 ka, 20 ka, and 5 ka (Figure 5; the latter identified from a Holocene section not shown) (Stevens and Lu, 2009). There is an apparent hiatus in the record from about 14 to 10 ka, interpreted previously as most likely caused by deflation during particularly arid and windy conditions (Lu *et al.*, 2006; Stevens *et al.*, 2006), followed by generally slow accumulation from about 10 ka to 5 ka. Similarly, accumulation rates at the other study sites show multiple and rather abrupt changes, although both the magnitude of the shifts and the absolute values are reduced compared with Huanxian. Significantly, the timing of these shifts varies considerably between all the sections (Huanxian, Xifeng, Xunyi and Lantian (Figure 2)), although there is a general reduction in accumulation rate from north-west to south-east. The gaps in the reconstructions at Xifeng, Xunyi and Lantian may be due to multiple OSL age inversions and frequent age underestimates at these points in the sections. This has been interpreted as caused by the effects of bioturbation during the formation of the Holocene soil in underlying glacial age material (Stevens *et al.*, 2006), meaning ages from these intervals cannot be used to calculate accumulation rate.

Despite the differences in timing and amplitude of the abrupt shifts in accumulation rate at the sites, averaged values tend to decrease into the Holocene, with the differences between the Holocene and last glacial becoming larger to the north-west. This pattern of variability has been interpreted as representing the importance of site specific conditions in determining accumulation rate on the Chinese Loess Plateau (Nugteren and Vandenberghe, 2004; Stevens and Lu, 2009).

Discussion

Timing of dune activity and stability

Although the use of OSL dating is well-established in aeolian research, there are important issues of interpretation in using this method to compare the timing of dune activity and loess accumulation. Dating of aeolian sand in dunefields typically produces a set of ages distributed unevenly over time. In previous work we have interpreted clusters of ages from aeolian sands as indicating periods of extensive dune activity (Lu *et al.*, 2005; Zhou *et al.*, 2008; Mason *et al.*, 2009). An alternative view is that a cluster of OSL ages from non-accumulating dunes must actually represent the time of dunefield *stabilization*, and that the main period of dune activity preceded the age cluster but are not represented by OSL dating because of continual recycling of sand (Chase and Thomas, 2006; Chase, 2009). This view clearly has implications for using OSL ages to test links between aeolian sand and loess systems.

We believe it is more plausible to interpret age clusters as indicating times of dune activity, not stabilization, particularly in semi-arid dunefields where turnover of sand is relatively slow; for example, in dunefields that are a mosaic of sand sheets and dune forms associated with some degree of vegetation cover, especially large compound parabolic dunes. We do recognize that OSL ages will probably be biased toward the young end of an extended period of dune activity, because of decreasing probability of preservation with increasing age. Furthermore, it is very likely that nonconformities produced by deflation occur at many sites, and the timing of dune activity

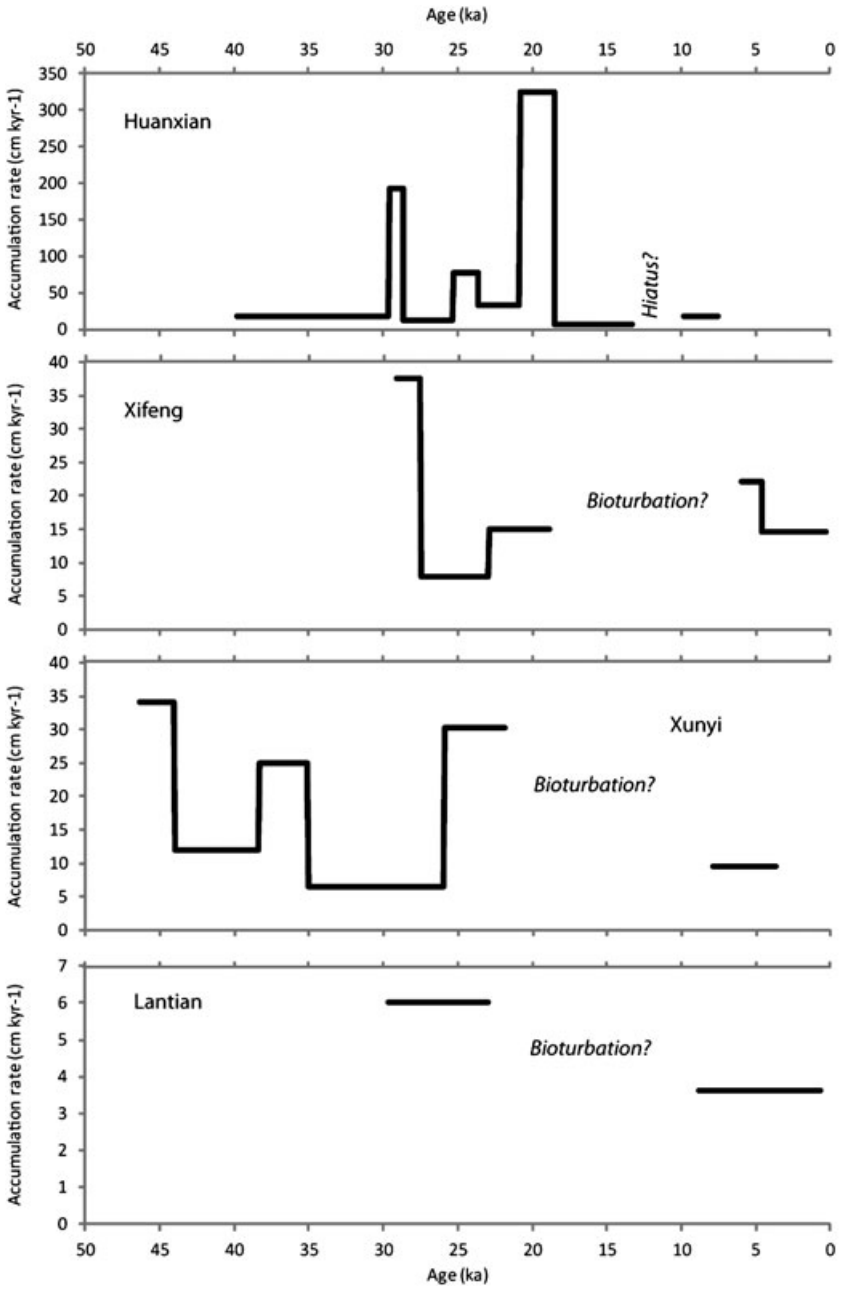

Figure 5. Dust accumulation rates estimated from closely spaced OSL dating at Huanxian (HX), Xifeng (XF), Xunyi (XY) and Lantian (LT) sites along a north-west–south-east transect in Chinese Loess Plateau (original data from Stevens and Lu, 2009).

and stability must be reconstructed by combining data from many sites. We recognize that interpretation of dunefield OSL ages remains an open issue; thus, we also consider implications for loess–aeolian sand linkage if dunefield ages are seen as times of stabilization, contrary to our preferred interpretation.

For the current study, the most important issue is whether OSL age clusters at 11–8 ka and <1 ka represent especially extensive dune activity, or times of stabilization. Modern observations in the especially active parts of the Otindag dunefield suggest an analogue for conditions in which sand was deposited at 11–8 ka. Sparsely vegetated surfaces display complex spatial patterns of erosion and deposition, and patches of denser vegetation locally stabilize sand, especially on the trailing arms of parabolic dunes. Active slipfaces are common on the larger dunes. In this setting, some sands are clearly reworked soon after deposition, while others may be preserved for much longer periods, for example where sand is buried within large dunes. Preservation of early and middle Holocene sand units and soils within relatively active modern large compound parabolic dunes of the Otindag dunefield supports the concept of a long turnover time in dunes of this type. Recycling of sand may be more rapid in the small active tranverse or barchanoid dunes that occur today in small patches of the Otindag dunefield (and larger parts of the other two study areas), but there is no clear evidence that these dune forms were common in the past.

Based on this analogy, there is no reason to assume that the period from 11 to 8 ka was characterized by progressive stabilization from an earlier, more active dunefield state; instead, the range of ages can be examples of spatial variation in turnover time of the sand, with some sand preserved for thousands of years within large slowly migrating dunes. Thus, we interpret the 11 to 8 ka age cluster as indicating a generally active dunefield state, with stabilization around 8 ka. It is possible that dune activity began before 11 ka but its initial stages are poorly represented by OSL dating. Two ages of 12.7 and 13.7 ka from the Mu Us dunefield (Table I, Figures 3 and 4) may support this hypothesis. Nonetheless, there is no positive

evidence of *greater* activity before 11 ka than between 11 ka and 8 ka, and no basis for assuming it must have occurred. As noted above, the dunefields may have apparently never expanded very far southward of their modern southern limits, and some sites with sands dated to 11–8 ka are very close to those limits.

Based on their context, the ages <1 ka represent widespread, though probably patchy aeolian activity which has continued to the present, and has involved fully mobile dunes. The small number of middle Holocene ages suggest that, although that time period was predominantly characterized by dune stability and soil development, activation and even substantial sand deposition did occur locally. This conclusion is consistent with the view that some of the thick middle Holocene soils contain multiple increments of sand deposited by minor aeolian activity.

Lack of coupling between dune activity and loess accumulation rates

The results provide little evidence to support the conceptual model of closely linked dunefield activity and loess accumulation rates at millennial and multi-millennial timescale, but also highlight the complex problems of interpretation that arise in making such a comparison. Rapid loess accumulation is recorded at intervals over the period 50 to 20 ka, broadly consistent with the hypothesis that loess accumulation increases during glacial periods. However, the detailed OSL dating indicates brief, millennial-scale intervals of high loess accumulation rate, varying in time between sections, rather a broader glacial peak of loess accumulation across the Loess Plateau.

No OSL ages from the dunefields indicate aeolian sand deposition between 50 and 20 ka, when episodes of rapid loess accumulation occurred (Figures 4a, 5). Although the simplest explanation of this observation is that extensive dune activity did not occur at that time, we cannot rule out the possibility that aeolian sand deposited at 50–20 ka was poorly preserved because of pervasive reworking during later dune activity, especially between 11 and 8 ka. Because active dunes were apparently near their long-term southern limit at 11–8 ka, however, the spatial extent of active dunefields was not substantially *greater* under glacial conditions at 50–20 ka than at 11–8 ka during the early Holocene. The alternative view that 11–8 ka was a period of stabilization would imply that peak dune activity occurred during some indefinite period ending around 11 ka, but the record from Huanxian clearly shows slow loess accumulation between 20 and 15 ka (Figure 5). Overall, the results generally contradict the traditional attribution of both peak loess accumulation rates and maximum desert expansion to reduced summer monsoon precipitation and strengthened winter monsoon winds under peak glacial conditions.

Unfortunately, it is difficult to estimate accumulation rates using OSL ages from the loess sections between about 14 and 9 ka, including the cluster of dune sand ages at 11–8 ka (Figure 4b, Figure 5). Large inversions suggest the record at many sites has been compromised by the effects of bioturbation or deflation. At Huanxian, the hiatus in accumulation between 14 and 10 ka has been tentatively attributed to deflation during a windy, arid period, as noted earlier (Lu *et al.*, 2006; Stevens *et al.*, 2006). That is, net removal of loess rather than rapid accumulation may have occurred at this site just prior to and during the episode of dune activity that began at 11 ka. However, more evidence is needed to test this hypothesis and the rate of accumulation during the subsequent period from 10 to 6 ka is low, contrasting with enhanced dune activity until 8 ka (Figure 4b, Figure 5). In fact, the most rapid Holocene loess accumulation is recorded at Huanxian at about 5 ka, a time of very limited dune activity. None of the loess sections record particularly high accumulation rates during the last 1000 years when dune activity was again extensive, although there is clear evidence of human impacts on loess stratigraphy at the top of the sequence at Lantian, and the record is truncated (again due to human agricultural practices) at Huanxian and Xunyi, making interpretations from this period difficult.

As discussed above, whether loess and aeolian sand systems respond independently to similar climatic controls or are directly linked by geomorphic processes, dune activity and rapid loess accumulation may not be synchronous *if* dust production is limited by sediment supply. Sediment supply effects could conceivably help reconcile our results with one or the other type of linkage between aeolian sand and loess systems, but only if we assume that widespread dune activity actually occurred between 50 and 20 ka but is not represented by our OSL ages because of poor preservation. If so, then dune activity and rapid loess accumulation might have initially occurred as expected, but loess source material was depleted in general (first type of linkage) or within the dunefields (second type). This scenario does not appear to merit further consideration without positive evidence for dune activity at 50–20 ka, however.

Overall, the lack of evidence for coupling between dune activity and loess accumulation is clear, despite the ambiguities in explaining this result. We suggest that any assumption of a consistent relationship between these aeolian systems should be cautious, until possible explanations for the lack of coupling can be more adequately evaluated.

Hypotheses on the lack of coupling between aeolian sand and loess systems

Geomorphic processes in the dunefields, especially the local erosion and redeposition of sand through dune migration, clearly must be considered in attempting to explain the apparent lack of coupling between aeolian systems, as discussed in the preceding two sections. In this section we propose two complementary hypotheses that can also explain our results, based on geomorphic processes involved in loess production and accumulation. First, site-specific conditions on the Loess Plateau and the dunefields may exert an overriding effect on aeolian deposition and accumulation, irrespective of dust production and emission. Second, much of the loess may be derived from sources upwind of the dunefields and is transported to the Loess Plateau without a storage phase within the dunes, and dust emission of those sources has climatic or other controls that differ from the factors influencing dune activity.

The first hypothesis is based on the lack of correspondence between accumulation rates at the four loess sites used in this study. Increasing numbers of other researchers have also found millennial-scale variations in loess accumulation rate, which do not appear to be consistent in timing at various sites on the Loess Plateau (Roberts *et al.*, 2001; Lai *et al.*, 2007; Buylaert *et al.*, 2008; Zhao *et al.*, 2008). Assuming that the sources of loess at the studied sites are broadly similar, this spatial variability implies that local influences exert a strong control on dust deposition and/or preservation. These site-specific factors may include local topography, vegetation and localized wind regimes (Pye, 1984). The availability of dust does not necessarily drive the accumulation of dust, and suitable means for trapping dust particles and preventing their subsequent deflation must be present in order for loess to accumulate. This

view is supported by modern observations that the Loess Plateau can act as both a dust source and sink at different times, depending on climate, surface conditions, and human disturbance (Quine *et al.*, 1997; Tang, 2000). Episodic water erosion and resedimentation of loess may also have affected these sites. It is to be expected therefore, that changes in local conditions can have a dramatic impact on the net accumulation of loess. Such changes may have created fine-scale hiatuses that are beyond the resolution of dating techniques.

In terms of the second hypothesis, modern observations confirm that large dust storms can be initiated within the Otindag and Mu Us dunefields, but are also common in more arid regions to the north and north-west (Lim and Chun, 2006; Shao and Dong, 2006). Provenance studies generally indicate that the Chinese loess has multiple and complex sources (Liu, 1964, 1985; Derbyshire, 1983; Liu *et al.*, 1993; Derbyshire *et al.*, 1998; Sun, 2002; Chen *et al.*, 2007). Vandenberghe *et al.* (2006) suggested that a substantial component of the loess comes directly from relatively distant western sources. This view is supported by a recent study using zircon ages, which concluded that some of the loess may be derived from the Mu Us dunefield, and possibly some sources further east, but more distant western sources make a major contribution (Stevens *et al.*, 2010). These provenance data allow the possibility that some of the loess may be derived either through sand-blasting of silt-rich source materials in the dunefields (e.g. sandy loess or lacustrine sediment), or abrasion of dune sand. However, the far-traveled component of the loess raises the possibility that temporal patterns of dust emission from source areas beyond the dunefields could strongly influence dust influx to the Loess Plateau. As discussed in the next section, there is good reason to believe that dust emission from those more distant sources may have had somewhat different climatic controls than dunefield activity, thus contributing to the lack of coupling between dune activity and loess accumulation rate.

Climatic controls on aeolian sand and loess systems

In this section, we consider a final set of explanations for the lack of coupling between dune activity and loess accumulation. First, the similarity of the broad patterns of late Quaternary climatic changes in the dunefields and other potential loess source regions is re-evaluated, using recent palaeoclimatic research. This is followed by discussion of reasons why aeolian sand and loess systems may have responded differently to those changes.

There is increasing evidence that many of the arid and semi-arid regions potentially supplying dust to the Loess Plateau did not experience late Quaternary changes in effective moisture (precipitation minus potential evapotranspiration, P-PET) that were in phase with variation of monsoon precipitation in central and southern China. Several recent papers have reviewed the evidence on Holocene palaeoclimates of northwestern China, Mongolia, and Central Asia, using a wide variety of palaeoclimatic indicators from many sites. These records generally indicate drier conditions in the early Holocene (*ca* 11–8 ka) than in the middle Holocene after 8 ka (Harrison *et al.*, 1996; Herzschuh, 2006; Chen *et al.*, 2008), though contrasting interpretations have been proposed for some areas (Ilyashuk and Ilyashuk, 2007). This temporal pattern of climatic change is quite different from that inferred from high-resolution speleothem records and other evidence in southern China, where peak monsoon precipitation apparently occurred in the early Holocene near the last maximum of Northern Hemisphere summer insolation, with declining precipitation after 8 ka (Wang *et al.*, 2005). We have previously proposed that the timing of aeolian sand activity in dunefields at the desert margin of northern China can be explained by assuming that this region also experienced the pattern of a drier early Holocene and wetter middle Holocene, as inferred for Central Asia and north-western China (Lu *et al.*, 2005; Mason *et al.*, 2009). That is, widespread dune activity before 8 ka primarily represents a response to lower effective moisture, followed by stabilization of the dunes by vegetation under wetter conditions after 8 ka.

Previous investigations have emphasized moisture as the most important factor influencing the stabilization and activation of dunes in northern China during the late Quaternary, at least before the onset of widespread human disturbance in the late Holocene (Dong *et al.*, 1983; Dong, 2002; Lu *et al.*, 2005; Sun *et al.*, 2006). The observation of older aeolian sands at a few sites suggests that activity between 11 and 8 ka may have largely reworked sand already present in the dunefields, although the role of external sediment supply clearly needs more investigation. Climatic factors such as wind strength or growing season length are likely to influence dryland dune activity, and there is good evidence from other semi-arid regions that the importance of moisture has been overemphasized (Chase, 2009; Chase and Brewer, 2009). Nonetheless, our recent work supports the view that effective moisture is the crucial factor in dunefields of northern China. The spatial pattern of dune activity in this region today is broadly consistent with control by effective moisture, with fully active dunefields limited to areas where annual average P-PET is less than about $-450\,\mathrm{mm\ yr^{-1}}$ (Mason *et al.*, 2009). While active dunes do occur in wetter climates, they are patchy and may often be attributable to human impacts (Mason *et al.*, 2008). Modern observations suggest the semiarid Mu Us, Horqin, and Otindag dunefields are not highly sensitive to changes in wind strength (Mason *et al.*, 2008). Large proportions of these dunefields (95–65% of test areas) remained stabilized by vegetation during a period of frequent strong winds and high potential sand transport in the 1970s (annual drift potential of 500–1700 vector units, Fryberger and Dean, 1979), and the patchy areas of active sand in those regions did not consistently shrink as wind strength dropped in subsequent decades (drift potentials below 300 vector units) (Mason *et al.*, 2008). While caution is needed in using this modern analogue study to understand the late Quaternary record, it provides the only available empirical data on response of these dunefields to changing wind strength.

Palaeoclimatic proxy data from Daihai Lake, between the Mu Us and Otindag dunefields, support the interpretation of dry climate in the dunefields during the early Holocene and a wetter climate beginning about 8 ka (Xiao *et al.*, 2004), revising the previous conclusion that the climate was wetter in the early Holocene (Wang *et al.*, 1990). Two other studies based on lake sediments north and north-west of the Mu Us dunefield also indicate a dry to wet transition in the early Holocene, although it is estimated to have occurred at 10 ka rather than 8 ka (Feng *et al.*, 2005; Yang *et al.*, 2010). A study of a lake north of the Mu Us dunefield suggests wetter conditions in the early Holocene and a dry middle Holocene, however (Chen *et al.*, 2003). Given the potential for site-specific factors to influence the record in individual lakes or dunefield stratigraphic sections, it is important to emphasize the general pattern from multiple sites and palaeoclimatic proxies, which at this time appears to indicate a dry early Holocene.

There is also some evidence of relatively dry conditions in the latest Pleistocene and early Holocene just to the south of the Mu Us dunefield in the Loess Plateau, using the new OSL-based timescales for the four loess sections used in this study to reconstruct climatic change from magnetic susceptibility and

grain-size distribution, as discussed above and illustrated in Figure 4a and b. Where loess is preserved just above or below the apparent hiatus at Huanxian within this time period, it has low magnetic susceptibility and coarse grain size, suggesting a dry climate and possibly stronger winds. Those conditions could also have reduced vegetation cover and allowed wind erosion that produced the hiatus itself. Loess dating between about 8.5 and 3 ka has higher magnetic susceptibility and finer grain size (Figure 2). At the other sites, Holocene bioturbation appears to have prevented the resolution of a detailed proxy record and overprinted on last glacial age loess, but the peak in Holocene magnetic susceptibility in the stacked record (Figure 4b) does not occur until the middle-late Holocene and proxy data taken from the bioturbated interval do not suggest increases in effective moisture earlier than this (Stevens and Lu, 2010). Following the accepted interpretation, this pattern indicates a weak summer monsoon (or more broadly, a dry climate) from 14 to about 8.5 ka, followed a wetter climate that reached a peak in the middle-late Holocene. Decreasing magnetic susceptibility suggests a shift back to a drier climate after about 3 ka, although there is not a similar shift to coarser grain size and the data from this time period may be affected by human land use.

To summarize, we propose that both the dunefields that we studied and the much larger area of northern China supplying dust to the Loess Plateau experienced similar latest Pleistocene to Holocene changes in effective moisture, which may not have co-varied with those in southern China. Furthermore, there is evidence from the OSL-dated loess sites that the moisture regime during the transition to the Holocene on the Loess Plateau may have been marked by a dry climate more similar to the dunefields than to southern China.

Importantly, dust emission from loess source areas would not necessarily have increased in response to the same climatic changes that triggered dune activity, so that loess accumulation and dune activity would not necessarily be coupled even in the absence of site-specific effects on loess accumulation. In particular, provenance data suggest that a substantial portion of the loess may ultimately be derived from the north-eastern Tibetan margin, probably the area around the Qilian Shan, probably through deflation of silt deposited on alluvial fans or in terminal basins along the northern margin of that mountain range (Lehmkuhl and Haselein, 2000; Stevens *et al.*, 2010). Thus, late Quaternary climatic change may have influenced dust production from these sources indirectly, through its complex effects on glaciation, hillslope erosion, and fluvial sediment yield in the Qilian Shan and other high, tectonically active, and glaciated mountains bordering desert basins of north-western China. Dust influx to the loess region may also be strongly influenced by wind regime. Modeling and modern observations emphasize the importance of strong winds in producing the dust storms that account for much of the total dust emission in northern China (e.g. Laurent *et al.*, 2006; Lim and Chun, 2006; Shao and Dong, 2006). Furthermore, Roe (2009) suggests that high rates of dust transport and loess accumulation should correspond to palaeoclimatic conditions favouring the formation of intense cyclones that generate strong surface winds. This challenges the current prevailing hypothesis that winter monsoon strength controlled by the Siberian high pressure system is responsible for driving shifts in dust transport and emission.

Conclusions

Comparison of OSL dated stratigraphic records of dunefield activity and loess accumulation rate reveals little evidence for synchronous change in these processes at millennial timescales in the late Quaternary, conflicting with the long-time held view that these two aeolian systems are tightly coupled. The loess accumulation rates estimated for sections in the Loess Plateau may reflect the complex interactions of sediment supply in the loess source areas, wind strength, and other climatic controls on dust production, and local factors influencing preservation of the loess after deposition. Variation of loess accumulation rates, at least at millennial timescales, cannot therefore be used as proxy evidence of changing monsoon system strength. However, it is important to note that our results do not necessarily conflict with patterns of broad-scale variation in loess accumulation rate exhibited over glacial–interglacial cycles, as extensively discussed in previous work (Liu and Ding, 1998; Xu *et al.*, 2007).

Variations in dunefield activity may have more straightforward controls, particularly effective moisture, but it cannot be assumed that these variations correspond directly to changes in strength of the Asian monsoon circulation. In fact, there is increasing evidence that effective moisture in the dunefields and a much broader region of northern China does not vary in phase with precipitation in the monsoon core region, and does not reach maximum levels during peaks of Northern Hemisphere summer insolation. This study highlights the importance of considering spatial variation in late Quaternary palaeoclimates, contrasting climatic and geomorphic controls on aeolian sand and loess systems, and local variation in the trapping and accumulation of dust as well as erosion, and preservation of the loess, when interpreting these important stratigraphic records of late Quaternary environmental change.

Acknowledgements—We thank Xianyan Wang, Lingjuan Wen, Cunfa Zhao, Xuefeng Sun, Xueqing Du, Chuanbin Yang, James B. Swinehart, Simon J. Armitage, David S.G. Thomas, Jan-Pieter Buylaert, Andrew S. Murray and Ronald J. Goble, Langping Li and Lin Zeng for their help in the field and laboratory, and paper preparation. This research is funded by National Natural Science Foundation of China (40930103, 40902045, 41021002), the MOST Global Changes Program (2010CB950203), US National Science Foundation (ATM-0502489, ATM-0502511, BCS-0352683, BCS-0352748), the UK-China Joint Project Grant of the Royal Society, and the Natural Environment Research Council (OSS/279/0205 and OSS/302/1105).

References

Bullard JE, McTainsh GH, Pudmenzky C. 2004. Aeolian abrasion and modes of fine particle production: an experimental study. *Sedimentology* **51**: 1103–1125.

Bullard JE, McTainsh GH, Pudmenzky C. 2007. Factors affecting the rate and nature of fine particle production by aeolian abrasion. *Sedimentology* **54**: 1169–1182.

Buylaert JP, Murray AS, Vandenberghe D, Vriend M, De Corte F, Van den haute P. 2008. Optical dating of Chinese loess using sand-sized quartz: establishing a time frame for Late Pleistocene climate changes in the western part of the Chinese Loess Plateau. *Quaternary Geochronology* **3**: 99–113.

Chase B. 2009. Evaluating the use of dune sediments as a proxy for palaeo-aridity: a southern African case study. *Earth Science Reviews* **93**: 31–45.

Chase B, Brewer S. 2009. Last Glacial Maximum dune activity in the Kalahari Desert of southern Africa: observations and simulations. *Quaternary Science Reviews* **28**: 301–307.

Chase B, Thomas DSG. 2006. Late Quaternary dune accumulation along the western margin of South Africa: distinguishing forcing mechanisms through the analysis of migratory dune forms. *Earth and Planetary Science Letters* **251**: 318–333.

Chen CT, Lan HC, Lou JY, Chen YC. 2003. The dry Holocene Megathermal in Inner Mongolia. *Palaeogeography, Palaeoclimatology, Palaeoecology* **193**: 181–200.

Chen FH, Yu ZC, Yang ML, Ito E, Wang SM, Madsen DB, Huang XZ, Zhao Y, Sato T, Birks JB, Boomer I, Chen JH, An CB, Wünnemann B. 2008. Holocene moisture evolution in arid central Asia and its out-of-phase relationship with Asian monsoon history. *Quaternary Science Reviews* **27**: 351–364.

Chen J, Li G, Yang J, Rao W, Lu H, Balsam W, Sun Y, Ji J. 2007. Nd and Sr isotopic characteristics of Chinese deserts: implications for the provenances of Asian dust. *Geochimica et Cosmochimica Acta* **71**: 3904–3914.

Crouvi O, Rivka A, Yehouda E, Naomi P, Amir S. 2008. Sand dunes as a major proximal dust source for late Pleistocene loess in the Negev Desert, Israel. *Quaternary Research* **70**: 275–282.

Derbyshire E. 1983. On the morphology, sediments and origin of the Loess Plateau of Central China. In *Megageomorphology*, Gardner R, Scoging H (eds). Oxford University Press: London; 172–194.

Derbyshire E, Meng XM, Kemp RA. 1998. Provenance, transport and characteristics of modern eolian dust in western Gansu Province, China, and interpretation of the Quaternary loess record. *Journal of Arid Environments* **39**: 497–516.

Ding ZL, Derbyshire E, Yang SL, Yu ZW, Xiong SF, Lui TS. 2002. Stacked 2.6-Ma grain-size record from the Chinese loess based on five sections and correlation with the deep-sea $\delta^{18}O$ record. *Paleoceanography* **17**: 1–21.

Dong GR. 2002. *Climate and Environment Changes in Deserts of China* (in Chinese). China Ocean Press: Beijing; 734.

Dong GR, Li BS, Gao SY, Wu Z, Shao YJ. 1983. The significance of the discovery of aeolian sand in Ordos Plateau during Quaternary. *Chinese Science Bulletin* **16**: 998–1001.

Feng ZD, Wang WG, Guo LL, Khosbayar P, Narantsetseg T, Jull AJT, An CB, Li XQ, Zhang HC, Ma YZ. 2005. Lacustrine and eolian records of Holocene climate changes in the Mongolian Plateau: preliminary results. *Quaternary International* **136**: 25–32.

Fryberger SG, Dean G. 1979. Dune forms and wind regime. In *A Study of Global Sand Seas*, McKee E (ed.), USGS Professional Paper 1052. US Geological Survey: Washington, DC.

Goble RJ, Mason JA, Loope DB, Swinehart JB. 2004. Optical and radiocarbon ages of stacked paleosols and dune sands in the Nebraska Sand Hills, USA. *Quaternary Science Reviews* **23**: 1173–1182.

Harrison SP, Yu G, Tarasov PE. 1996. Late Quaternary lake-level record from northern Eurasia. *Quaternary Research* **45**: 138–159.

Herzschuh U. 2006. Palaeo-moisture evolution in monsoonal Central Asia during the last 50,000 years. *Quaternary Science Reviews* **25**: 163–178.

Ilyashuk BP, Ilyashuk EA. 2007. Chironomid record of Late Quaternary climatic and environmental changes from two sites in Central Asia (Tuva Republic, Russia)--local, regional or global causes? *Quaternary Science Reviews* **26**: 705–731.

Kohfeld KE, Harrison SP. 2003. Glacial-interglacial changes in dust deposition on the Chinese Loess Plateau. *Quaternary Science Reviews* **22**: 1859–1878.

Lai ZP, Wintle AG, Thomas DSG. 2007. Rates of dust deposition between 50 ka and 20 ka revealed by OSL dating at Yuanbao on the Chinese Loess Plateau. *Palaeogeography, Palaeoclimatology, Palaeoecology* **248**: 431–439.

Laurent B, Marticorena B, Bergametti G, Mei F. 2006. Modeling mineral dust emissions from Chinese and Mongolian deserts. *Global and Planetary Change* **52**: 121–141.

Lehmkuhl F, Haselein F. 2000. Quaternary paleoenvironmental change on the Tibetan Plateau and adjacent areas (Western China and Western Mongolia). *Quaternary International* **65/66**: 121–145.

Li LP, Lu HY. 2010. A preliminarily quantitative estimation of the sedimentation and erosion rates of loess deposits in Chinese Loess Plateau over the past 250 ka based on geostatistics and remote sensing analyses. *Acta Geographica Sinica* **65**(1): 37–52.

Li SH, Sun JM, Zhao H. 2002. Optical dating of dune sands in the northeastern deserts of China. *Palaeogeography, Palaeoclimatology, Palaeoecology* **181**: 419–429.

Lim JY, Chun Y. 2006. The characteristics of Asian dust events in Northeast Asia during the springtime from 1993 to 2004. *Global and Planetary Change* **52**: 231–247.

Liu CQ, Masuda A, Okada A, Yabuki S, Zhang J, Fan ZL. 1993. A geochemical study of loess and desert sand in northern China: implications for continental crust weathering and composition. *Chemical Geology* **196**: 359–374.

Liu TS. 1964. *The Loess in the Middle Reach of the Yellow River*. Science Press: Beijing.

Liu TS. 1985. *Loess and the Environment*. China Ocean Press: Beijing.

Liu TS, Ding ZL. 1998. Chinese loess and the paleomonsoon. *Annual Reviews of Earth and Planetary Sciences* **26**: 111–145.

Lu HY, An ZS. 1998. Palaeoclimatic significance of grain size of loess-palaeosol deposit in Chinese Loess Plateau. *Sciences in China Series D* **41**: 626–631.

Lu HY, Miao XD, Zhou YL, Mason J, Swinehart J, Zhang JF, Zhou LP, Yi SW. 2005. Late Quaternary aaeolian activity in the Mu Us and Otindag dunefields (North China) and lagged response to insolation forcing. *Geophysical Research Letters* **32**: L21716.

Lu HY, Stevens T, Yi SW, Sun XF. 2006. An erosional hiatus in Chinese loess sequences revealed by closely spaced optical dating. *Chinese Science Bulletin* **51**: 2253–2259.

Lu YC, Wang XL, Wintle AG. 2007. A new OSL chronology for dust accumulation in the last 130,000 yr for the Chinese Loess Plateau. *Quaternary Research* **67**(1): 152–160.

Ma J, Yue LP, Yang LR, Sun L, Xu Y. 2011. OSL dating of Holocene sequence and palaeoclimate change record in southeastern margin if Mu Us desert, North China. *Quaternary Sciences* **31**(1): 120–129.

Maher BA, Hu M. 2006. A high-resolution record of Holocene rainfall variations from the western Chinese Loess Plateau: antiphase behavior of the African/Indian and East Asian summer monsoons. *The Holocene* **16**: 309–319.

Mason JA, Swinehart JB, Lu HY, Miao XD, Cha P, Zhou YL. 2008. Limited change in dune mobility in response to a large decrease in wind power in semi-arid northern China since the 1970s. *Geomorphology* **102**: 351–363.

Mason JA, Lu HY, Zhou YL, Miao X, Swinehart JB, Liu ZY, Goble RJ, Yi SW. 2009. Dune mobility and aridity at the desert margin of northern China at a time of peak monsoon strength. *Geology* **37**: 947–950.

Murray AS, Marten R, Johnston A, Martin P. 1987. Analysis for naturally occurring radionuclides at environmental concentrations by gamma spectrometry. *Journal of Radioanalytical and Nuclear Chemistry* **115**: 263–288.

Murray AS, Wintle AG. 2003. The single aliquot regenerative dose protocol: potential for improvements in reliability. *Radiation Measurements* **37**: 377–381.

Nickling WG, Gillies JA. 1989. Emission of fine-grained particulates from desert soils. In *Paleoclimatology and Paleometeorology: Modern and Past Patterns of Global Atmospheric Transport*, Leinen M, Sarnthein M (eds). Kluwer Academic Publishers: Norwell, MA; 133–166.

Nugteren GD, Vandenberghe J. 2004. Spatial climatic variability on the Central Loess Plateau (China) as recorded by grain size for the last 250 kyr. *Global and Planetary Change* **41**: 185–206.

Porter SC. 2001. Chinese loess record of monsoon climate during the last glacial-interglacial cycle. *Earth Science Review* **54**: 115–128.

Prescott JR, Hutton JT. 1994. Cosmic ray contribution to dose rates for luminescence and ESR dating: large depths and long-term time variations. *Radiation Measurements* **23**: 497–500.

Pye K. 1984. Loess. *Progress in Physical Geography* **8**: 176–217.

Quine TA, Govers G, Walling DE, Zhang XB, Desmet PJJ, Zhang YS, Vandaele K. 1997. Erosion processes and landform evolution on agricultural land-new perspective from caesium-137 measurements and topographic-based erosion. *Earth Surface Processes and Landforms* **22**: 799–816.

Roberts HM, Wintle AG, Maher BA, Hu MY, 2001. Holocene sediment-accumulation rates in the western Loess Plateau, China, and a 2500-year record of agricultural activity, revealed by OSL dating. *The Holocene* **11**: 477–485.

Roe G. 2009. On the interpretation of Chinese loess as a palaeoclimate indicator. *Quaternary Research* **71**(2): 150–161.

Shao Y, Raupach M, Findlater M. 1993. Effect of saltation bombardment on the entrainment of dust by wind. *Journal of Geophysical Research* **98**: 12719–12726.

Shao Y, Dong CH. 2006. A review on East Asian dust storm climate, modeling and monitoring. *Global and Planetary Change* **52**: 1–22.

Smalley IJ, Vita-Frinzi C. 1968. The formation of fine particles in sand deserts and the nature of 'desert' loess. *Journal of Sedimentary Petrology* **38**: 766–774.

Stevens T, Armitage SJ, Lu HY, Thomas DSG. 2006. Sedimentation and diagenesis of Chinese loess: implications for the preservation of continuous high-resolution climate records. *Geology* **34**: 849–852.

Stevens T, Lu HY. 2009. Optical stimulated luminescence dating as a tool for calculating sedimentation rates in Chinese loess: comparisons to grain-size records. *Sedimentology* **56**: 911–934.

Stevens T, Lu HY. 2010. Radiometric dating of the late Quaternary summer monsoon on the Loess Plateau, China. In *Monsoon Evolution and Tectonics-Climate Linkage in Asia*, Vol. **342**, Clift PD, Tada R, Zheng H (eds). Geological Society: London, Special Publication; 87–108.

Stevens T, Lu HY, Thomas DSG, Armitage SJ. 2008. Optical dating of abrupt shifts in the Late Pleistocene East Asian monsoon. *Geology* **36**: 415–418.

Stevens T, Palk C, Carter A, Lu HY, Clift PD. 2010. Assessing the provenance of loess and desert sediments in northern China using U-Pb dating and morphology of detrital zircons. *Geological Society of America Bulletin* **122**: 1331–1344.

Sun JM. 2002. Source regions and formation of the loess sediments on the high mountain regions of Northwestern China. *Quaternary Research* **58**: 341–351.

Sun JM, Li SH, Han P, Chen Y. 2006. Holocene environmental changes in the central Inner Mongolia, based on single-aliquot-quartz optical dating and multi-proxy study of dune sands. *Palaeogeography, Palaeoclimatology, Palaeoecology* **233**: 51–62.

Tang KL. 2000. Significance and pressure on protection of water-wind erosion region in the Loess Plateau. *Soil and Water Conservation in China* (in Chinese) **11**: 1–12.

Vandenberghe J, Renssen H, van Huissteden K, Nugteren G, Konert M, Lu HY, Dodonov A, Buylaert JP. 2006. Penetration of Atlantic westerly winds into Central and East Asia. *Quaternary Science Reviews* **25**: 2380–2389.

Wang SM, Wu RJ, Jiang XH. 1990. Environment evolution and paleoclimate of Daihai Lake, Inner Mongolia since the last glaciation. *Quaternary Sciences* **3**: 223–232.

Wang Y, Cheng H, Edwards RL, He YQ, Kong XG, An ZS, Wu JY, Kelly MJ, Dykoski CA, Li XD. 2005. The Holocene Asian monsoon; links to solar changes and North Atlantic climate. *Science* **308**: 854–857.

Wright JS. 2001. 'Desert' loess versus 'glacial' loess: quartz silt formation, source areas and sediment pathways in the formation of loess deposits. *Geomorphology* **36**: 231–256.

Wright JS. 2007. An overview of the role of weathering in the production of quartz silt. *Sedimentary Geology* **202**: 337–351.

Wright JS, Smith BJ, Whalley WB. 1998. Mechanisms of loess-sized quartz silt production and their relative effectiveness: laboratory simulations. *Geomorphology* **23**: 15–34.

Xiao JL, Xu Q, Nakamura T, Yang X, Liang W, Inouchi Y. 2004. Holocene vegetation variation in the Daihai Lake region of north-central China: a direct indication of the Asian monsoon climatic history. *Quaternary Science Reviews* **23**: 1669–1679.

Xu SJ, Pan BT, Gao HS, Cao GJ, Su H. 2007. Changes in sand fractions of Binggou section and the expansion and contraction of the Tengger Desert during 50–30 ka. *Earth Surface Processes and Landforms* **32**: 475–480.

Yang XP, Rost KT, Lehmkuhl F, Zhu Z, Dodson J. 2004. The evolution of dry lands in northern China and the Republic of Mongolia since the Last Glacial Maximum. *Quaternary International* **118–119**: 69–85.

Yang XP, Ma N, Dong JF, Zhu BQ, Xu B, Ma ZB, Liu JQ. 2010. Recharge to the inter-dune lakes and Holocene climatic changes in the Badain Jaran Desert, western China. *Quaternary Research* **73**: 10–19.

Yang XP, Zhu B, Wang X, Li C, Zhou Z, Chen J, Wang X, Yin J, Lu Y. 2008. Late Quaternary environmental changes and organic carbon density in the Hunshandake Sandy Land, eastern Inner Mongolia, China. *Global and Planetary Change* **61**: 70–78.

Zhao H, Chen FH, Li SH, Wintle AG, Fan YX, Xia DS. 2008. A record of Holocene climate change in the Guanzhong Basin, China, based on optical dating of a loess-palaeosol sequence. *The Holocene* **17**: 1015–1022.

Zhou YL, Lu HY, Mason J, Miao XD, Swinehart J, Goble R. 2008. Optically stimulated luminescence dating of aaeolian sand in the Otindag dunefield and Holocene climate change. *Science in China Series D* **51**: 837–847.

Zhou YL, Lu HY, Zhang JF, Mason J, Zhou LP. 2009. Luminescence dating of sand -loess sequences and response of Mu Us and Otindag sand fields (north China) to climatic changes. *Journal of Quaternary Science* **24**: 336–344.